Mapping dynamic environments using Markov random field models

Hongjun Li[1], Miguel Barão[2] and Luís Rato[1]
[1]Department of Informatics, University of Evora, Evora, Portugal
[2]Research Centre for Mathematics and Applications, University of Evora, Evora, Portugal
li.hongjun@foxmail.com, mjsb@uevora.pt, lmr@uevora.pt

***Abstract*—This paper focuses on dynamic environments for mobile robots and proposes a new mapping method combining hidden Markov models (HMMs) and Markov random fields (MRFs). Grid cells are used to represent the dynamic environment. The state change of every grid cell is modelled by an HMM with an unknown transition matrix. MRFs are applied to consider the dependence between different transition matrices. The unknown parameters are learnt from not only the corresponding observations but also its neighbours. Given the dependence, parameter maps are smooth. Expectation Maximum (EM) is applied to obtain the best parameters from observations. Finally, a simulation is done to evaluate the proposed method.**

***Keywords*—Hidden Markov models, Grid map, Markov random fields.**

I. Introduction

The earlier research for mobile robots is developed under the static environment assumption. However, in real environments, there are dynamic objects such as people and doors. Dynamic objects move randomly and it is not easy to know their next positions precisely. Object tracking is to estimate the positions and velocities of dynamic objects. The estimation provides instant information of dynamic objects and the robot can plan its next step in order to avoid collisions.

Another representative model for dynamic environments is HMM [1]. HMM is applied to model the dynamic environments in [2]. The map is divided into grid cells [3] and an HMM is applied to model every grid cell. Every grid cell has two possible states: occupied and free. The state change of one grid cell is represented by a transition matrix. One grid cell may also be observed occupied or free. In addition, the grid cell is unknown when it is outside the measurement. Given the measurements obtained by sensors, the transition matrix can be learnt. In [4], there are three possible observations: true, false and not observable. However, the underlying possible states are extended and consist of seven components: true, false, unknown, dynamic, falsely false, false true, falsely true/false. The last three are used to deal with wrong observations. HMM is applied to classify dynamic objects such as adults, cars and dogs [5]. The transition probabilities are learnt from a clustered exemplar set and can be used to classify tracks of different objects in a Bayesian filtering framework. The dynamic maps based on HMM are used to do lifelong localization task in [6] and simultaneous localization and mapping in [7]. The observations of neighbour cells in the previous time step are considered in [8] and it is modelled as an input-output hidden Markov model (IOHMM) [9]. The current state of one grid cell depends on not only its previous state but also the previous observations of its neighbours. In this manner, the spatial correlation is considered. The Explicit-state-Duration Hidden Markov Model (EDHMM) is applied to differentiate the dynamic cells from static environment [10]. The duration between two states is variable.

In this paper, we propose a new mapping method for dynamic environments, which combines HMMs and MRFs. The dynamic environment is divided into grid cells and an HMM is also applied to model every grid cell. The transition matrices in HMMs are unknown parameters. The dependence between different transition matrices is considered by MRFs to ensure smooth estimation. HMMs are introduced in Section II. One grid cell is associated with two parameters and one map is represented by two parameter maps. In Section III, the proposed method is presented under the assumption that two parameter maps are independent. Two parameter maps are regarded as two independent MRFs. The MRF model is built in Section III-A. EM for the MRF model is applied to learn the parameters in Section III-B. The simulation is described in Section IV.

II. HMMs for dynamic environments

The map is divided into many grid cells and every grid cell at coordinate c have two possible states: occupied and free, which are denoted s_1 and s_2. In dynamic environments, the states of some grid cells may change over time. The changes can be modelled as Markov chains. A Markov chain can be specified by a transition matrix as

$$A_c = \begin{bmatrix} a_{11}^c & 1-a_{11}^c \\ 1-a_{22}^c & a_{22}^c \end{bmatrix}, \tag{1}$$

where $a_{11}^c = p(m_c^{t+1} = s_1 \mid m_c^t = s_1)$ represents the probability of state staying occupied from time t to time $t+1$ and $a_{22}^c = p(m_c^{t+1} = s_2 \mid m_c^t = s_2)$ represents the probability of state staying free. In our work, a laser sensor is used to precept the environment. Because of the uncertainty of the sensor, the state cannot be measured precisely. Following along a laser beam in the measurement direction, the grid cells are free at least until the measured distance. At the end of the measurement range, the cell is occupied. When the measurement range is the maximum range of laser beam, all the grid cells covered by the laser beam are free. One grid

This work was supported by EACEA under the Erasmus Mundus Action 2, Strand 1 project LEADER - Links in Europe and Asia for engineering, eDucation, Enterprise and Research exchanges.

cell is not observed all the time. The observation model can be specified by

$$B = \begin{bmatrix} p(z \mid m_c^t = s_1) & 0 \\ 0 & p(z \mid m_c^t = s_2) \end{bmatrix}, \quad (2)$$

where $z \in \{occupied, free, unobserved\}$ [2].

The observation model is known. In order to estimate the transition matrix, the initial probabilities $\rho_1^c = p(m_c^0 = s_1)$ and $\rho_2^c = p(m_c^0 = s_2)$ are required. The parameters for an HMM are denoted $\theta_c = \{a_{11}^c, a_{22}^c, \rho_1\}$. Assume the observation sequence is $O_c = \{y_c^0, y_c^1, \cdots, y_c^\zeta\}$ and a underlying state sequence $\mathcal{M}_c$. The joint distribution of observations and an underlying state sequence is

$$\begin{aligned} &p(O_c, \mathcal{M}_c \mid \theta_c) \\ &= p(m_c^0) p(z^0 \mid m_c^0) \prod_{t=1}^{\zeta} p(m_c^t \mid m_c^{t-1}) \prod_{t=1}^{\zeta} p(y^t \mid m_c^t), \end{aligned} \quad (3)$$

The parameters can be estimated by maximum likelihood as

$$\hat{\theta}_c = \arg\max_{\theta} \sum_{\mathcal{M}_c} p(O_c, \mathcal{M}_c \mid \theta_c). \quad (4)$$

However, it is not feasible to maximize the likelihood directly. Baum-Welch algorithm can be applied to estimate the parameters by maximizing a Q function, which is given as

$$\begin{aligned} &Q(\theta_c, \theta_c^{(k)}) = \sum_{\mathcal{M}_c} p(\mathcal{M}_c \mid O_c, \theta_c^{(k)}) \log p(\mathcal{M}_c, O_c \mid \theta_c) \\ &= \sum_{\mathcal{M}_c} p(\mathcal{M}_c \mid O_c, \theta_c^{(k)}) \left(\log p(O_c \mid \mathcal{M}_c, \theta_c) + \log p(\mathcal{M}_c \mid \theta_c) \right) \\ &= \sum_{\mathcal{M}_c} p(\mathcal{M}_c \mid O_c, \theta_c^{(k)}) \log p(O_c \mid \mathcal{M}_c, \theta_c) \\ &+ \sum_{\mathcal{M}_c} p(\mathcal{M}_c \mid O_c, \theta_c^{(k)}) \log p(\mathcal{M}_c \mid \theta_c). \end{aligned} \quad (5)$$

Given the state sequence $\mathcal{M}_c$, the observation sequence O_c does no depend on the parameters θ_c. $p(O_c \mid \mathcal{M}_c, \theta_c)$ can be rewritten as $p(O_c \mid \mathcal{M}_c)$, which can be derived from the observation probabilities. Because the observation probabilities are known, the first item is a constant in (5). Focus on the second one, we can obtain

$$\begin{aligned} &\sum_{\mathcal{M}_c} p(\mathcal{M}_c \mid O_c, \theta_c^{(k)}) \log p(\mathcal{M}_c \mid \theta_c) \\ &= \sum_{i=1}^{2} \gamma_i^c(0) \log \rho_i^c + \sum_t \sum_{i=1}^{2} \xi_{1i}^c(t) \log a_{1i}^c + \sum_t \sum_{i=1}^{2} \xi_{2i}^c(t) \log a_{2i}^c \\ &= f(\rho_1^c) + f(a_{11}^c) + f(a_{22}^c), \end{aligned} \quad (6)$$

where

$$\begin{aligned} f(\rho_1^c) &= \sum_{i=1}^{2} \gamma_i^c(0) \log \rho_i^c \\ &= \gamma_1^c(0) \log \rho_1^c + \gamma_2^c(0) \log(1 - \rho_1^c), \end{aligned} \quad (7)$$

$$\begin{aligned} f(a_{11}^c) &= \sum_t \sum_{i=1}^{2} \xi_{1i}^c(t) \log a_{1i}^c \\ &= \sum_t \xi_{11}^c(t) \log a_{11}^c + \sum_t \xi_{12}^c(t) \log(1 - a_{11}^c), \end{aligned} \quad (8)$$

$$\begin{aligned} f(a_{22}^c) &= \sum_t \sum_{i=1}^{2} \xi_{2i}^c(t) \log a_{2i}^c \\ &= \sum_t \xi_{21}^c(t) \log(1 - a_{22}^c) + \sum_t \xi_{22}^c(t) \log a_{22}^c, \end{aligned} \quad (9)$$

and $\gamma_i^c(t) = p(m_c^t = s_i \mid O_c, \theta_c^{(k)})$ is the probability of being in state s_i at time t given the observed sequence O_c and the parameters $\theta_c^{(k)}$, $\xi_{ij}^c(t) = p(m_c^t = s_i, m_c^{t+1} = s_j \mid O_c, \theta_c^{(k)})$ is the probability of being in state s_i at time t and state s_j at time $t+1$ given the observed sequence O_c and parameters $\theta_c^{(k)}$. $\gamma_i^c(t)$ and $\xi_{ij}^c(t)$ can be computed as the forward process and backward process in Baum-Welch algorithm. The parameters can be updated as

$$\rho_i^{c(k+1)} = \gamma_i^c(0), \quad (10)$$

$$a_{ij}^{c(k+1)} = \frac{\sum_{t=1}^{\zeta} \xi_{ij}^c(t)}{\sum_{t=1}^{\zeta} \gamma_i^c(t)}. \quad (11)$$

III. Proposed method

A. The MRF model

The set of a_{11}^c and a_{22}^c for all the grid cells are denoted $\boldsymbol{A} = (\boldsymbol{a}_1, \boldsymbol{a}_2)$, where $\boldsymbol{a}_1 = [\cdots, a_{11}^c, \cdots]^{\mathrm{T}}$ and $\boldsymbol{a}_2 = [\cdots, a_{22}^c, \cdots]^{\mathrm{T}}$. $\boldsymbol{a}_1$ and $\boldsymbol{a}_2$ are assumed to be independent. The prior distribution can be factorized as

$$p(\boldsymbol{A}) = p(\boldsymbol{a}_1) p(\boldsymbol{a}_2). \quad (12)$$

The dependence between different a_{11} and the dependence between different a_{22} are considered individually. $\boldsymbol{a}_1$ is taken as an example to show how to formulate the dependence. The log odds form of a_{11}^c is defined as

$$l_{a_{11}}^c = \log \frac{a_{11}^c}{1 - a_{11}^c}. \quad (13)$$

Assume the vector of all the $l_{a_{11}}^c$ is regarded as an MRF and denoted $l_{a_1} = [\cdots, l_{a_{11}}^c, \cdots]^{\mathrm{T}}$. A second-order neighbourhood system in this MRF, which includes the diagonal grid cells, is shown as Figure 1. Every random variable l_{a11}^c has eight neighbours denoted $l_{a11}^{c'}$.

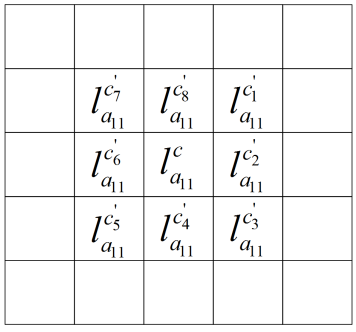

Fig. 1: A second-order neighbourhood system in an MRF

A clique C is defined as a subset of variables that are neighbours to one another. The pair-variable cliques are shown in Figure 2. The collection of the pair-variable cliques is denoted C_2. In one second-order neighbourhood, there are eight pair-variable cliques.

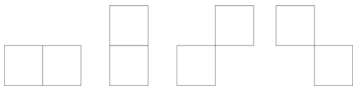

Fig. 2: Pair-variable cliques in second-order neighbourhood system

Only the pair-variable cliques in the second-order neighbourhood systems are considered. The prior probability is

$$p(l_{a_1}) = \frac{1}{Z}\exp(-\frac{1}{\mathcal{T}}\sum_{C\in C_2} V_C(l_{a_1})), \tag{14}$$

where

$$Z = \sum_{l_{a_1}} \exp(-\frac{1}{\mathcal{T}}\sum_{C\in C_2} V_C(l_{a_1})), \tag{15}$$

$\mathcal{T}$ is the temperature, $V_C(l_{a_1})$ is the clique potential and defined as

$$V_C(l_{a_1}) = (l^c_{a_{11}} - l^{c'}_{a_{11}})^2. \tag{16}$$

Expand these clique potentials, the sum in (14) is quadratic. The prior can be rewritten as

$$p(l) = \frac{1}{Z}\exp(-\frac{2}{\mathcal{T}} l^{\mathrm{T}}_{a_1}\mathcal{A} l_{a_1}). \tag{17}$$

The prior distribution $p(\boldsymbol{a_1})$ is

$$p(\boldsymbol{a}_1) = \frac{1}{Z}\exp\left(-\frac{1}{\mathcal{T}}U(\boldsymbol{a}_1)\right), \tag{18}$$

where

$$U(\boldsymbol{a}_1) = 2(\log\frac{\boldsymbol{a}_1}{\mathbf{1}-\boldsymbol{a}_1})^{\mathrm{T}}\mathcal{A}\log\frac{\boldsymbol{a}_1}{\mathbf{1}-\boldsymbol{a}_1}. \tag{19}$$

$\mathbf{1}$ is a column of ones. Similarly, the log odds form of a^c_{22} is defined as

$$l^c_{a_{22}} = \log\frac{a^c_{22}}{1-a^c_{22}}. \tag{20}$$

Assume the vector of all the $l^c_{a_{22}}$ is also regarded as an MRF and denoted $l_{a_2} = [\cdots, l^c_{a_{22}}, \cdots]^{\mathrm{T}}$. $p(\boldsymbol{a}_2)$ is given as

$$p(\boldsymbol{a}_2) = \frac{1}{Z}\exp\left(-\frac{1}{\mathcal{T}}U(\boldsymbol{a}_2)\right), \tag{21}$$

where

$$U(\boldsymbol{a}_2) = 2(\log\frac{\boldsymbol{a}_2}{\mathbf{1}-\boldsymbol{a}_2})^{\mathrm{T}}\mathcal{A}\log\frac{\boldsymbol{a}_2}{\mathbf{1}-\boldsymbol{a}_2}. \tag{22}$$

$\boldsymbol{a}_1$ and $\boldsymbol{a}_2$ have the same configuration space. The normalizers in two different distributions are the same as Z.

The coordinate set of observed grid cells is denoted $\mathcal{I}$ and the observation set $O = \{O_c\}$ $(c \in \mathcal{I})$ consists all the observation sequences O_c of observed grid cells. A underlying configuration sequence is denoted $\mathcal{M} = \{\mathcal{M}_c\}$ $(c \in \mathcal{I})$, which consists of all the underlying state sequences of observed grid cells. In probabilistic form, the likelihood is $p(O \mid \boldsymbol{A})$. The joint probability $p(O, \mathcal{M} \mid \boldsymbol{A})$ is

$$p(O, \mathcal{M} \mid \boldsymbol{A}) = p(O \mid \mathcal{M}, \boldsymbol{A})p(\mathcal{M} \mid \boldsymbol{A}). \tag{23}$$

Assume all the observation sequences are dependent of each other, it is rewritten as

$$p(O, \mathcal{M} \mid \boldsymbol{A}) = \prod_{c\in\mathcal{I}} p(O_c \mid \mathcal{M}_c, A_c)p(\mathcal{M}_c \mid A_c), \tag{24}$$

where $p(O_c \mid \mathcal{M}_c, A_c)$ is the same as $p(O_c \mid \mathcal{M}_c, \theta_c)$ and $p(\mathcal{M}_c \mid A_c)$ is the same as $p(\mathcal{M}_c \mid \theta_c)$. For convenience, A_c is used instead. The likelihood can be given as

$$p(O \mid \boldsymbol{A}) = \sum_{\mathcal{M}} p(O, \mathcal{M} \mid \boldsymbol{A}) \tag{25}$$

Based on Bayes rule, the posterior distribution is

$$p(\boldsymbol{A} \mid O) = \frac{p(O \mid \boldsymbol{A})p(\boldsymbol{A})}{p(O)}, \tag{26}$$

where $p(O)$ is a constant.

B. EM

Maximizing $p(\boldsymbol{A} \mid O)$, the best estimation can be obtained. Equivalently we need to maximizing

$$p(O, \boldsymbol{A}) = p(O \mid \boldsymbol{A})p(\boldsymbol{A}). \tag{27}$$

This problem is similar to the HMM without prior and it is not possible to search the maximum directly. EM algorithm is applied to solve this problem. In E step, the Q function is given as

$$\begin{aligned} &Q(\boldsymbol{A}, \boldsymbol{A}^{(k)}) = E_{\mathcal{M}|O,\boldsymbol{A}^{(k)}}\log p(\mathcal{M}, O \mid \boldsymbol{A}) + \log p(\boldsymbol{A}) \\ &= E_{\mathcal{M}|O,\boldsymbol{A}^{(k)}}\log p(O \mid \mathcal{M}, \boldsymbol{A}) + E_{\mathcal{M}|O,\boldsymbol{A}^{(k)}}\log p(\mathcal{M} \mid \boldsymbol{A}) \\ &- 2\log Z - \frac{1}{\mathcal{T}}U(\boldsymbol{a}_1) - \frac{1}{\mathcal{T}}U(\boldsymbol{a}_2). \end{aligned} \tag{28}$$

$p(O \mid \mathcal{M}, \boldsymbol{A})$ can be rewritten as $p(O \mid \mathcal{M})$. The first term and $\log Z$ are constants. Discarding the constant parts gives

$$\begin{aligned} &E_{\mathcal{M}|O,\boldsymbol{A}^{(k)}}\log p(\mathcal{M} \mid \boldsymbol{A}) - \frac{1}{\mathcal{T}}U(\boldsymbol{a}_1) - \frac{1}{\mathcal{T}}U(\boldsymbol{a}_2) \\ &= \sum_{\mathcal{M}} p(\mathcal{M} \mid O, \boldsymbol{A}^{(k)}) \sum_{c\in\mathcal{I}} \log p(\mathcal{M}_c \mid A_c) - \frac{1}{\mathcal{T}}U(\boldsymbol{a}_1) - \frac{1}{\mathcal{T}}U(\boldsymbol{a}_2) \\ &= \sum_{c\in\mathcal{I}}\sum_{\mathcal{M}} p(\mathcal{M} \mid O, \boldsymbol{A}^{(k)})\log p(\mathcal{M}_c \mid A_c) - \frac{1}{\mathcal{T}}U(\boldsymbol{a}_1) - \frac{1}{\mathcal{T}}U(\boldsymbol{a}_2) \\ &= \sum_{c\in\mathcal{I}}\sum_{\mathcal{M}_c} p(\mathcal{M}_c \mid O, \theta^{(k)}_c)\log p(\mathcal{M}_c \mid A_c) - \frac{1}{\mathcal{T}}U(\boldsymbol{a}_1) - \frac{1}{\mathcal{T}}U(\boldsymbol{a}_2). \end{aligned} \tag{29}$$

Based on (6), this expectation is rewritten as

$$\begin{aligned} &E_{\mathcal{M}|O,\boldsymbol{A}^{(k)}}\log p(\mathcal{M} \mid \boldsymbol{A}) - \frac{1}{\mathcal{T}}U(\boldsymbol{a}_1) - \frac{1}{\mathcal{T}}U(\boldsymbol{a}_2) \\ &= \sum_{c\in\mathcal{I}} f(\rho^c_1) + \sum_{c\in\mathcal{I}} f(a^c_{11}) + \sum_{c\in\mathcal{I}} f(a^c_{22}) - 2U(\boldsymbol{a}_1) - 2U(\boldsymbol{a}_2) \\ &= f(\boldsymbol{\rho}_1) + f(\boldsymbol{a}_1) + f(\boldsymbol{a}_2), \end{aligned} \tag{30}$$

where the set of initial occupancy probabilities of observed grid cells is denoted $\boldsymbol{\rho}_1 = [\cdots, \rho^c_1, \cdots]^{\mathrm{T}}$ $(c \in \mathcal{I})$. The three functions $f(\boldsymbol{\rho}_1)$, $f(\boldsymbol{a}_1)$ and $f(\boldsymbol{a}_2)$ are defined as

$$\begin{aligned} f(\boldsymbol{\rho}_1) &= \sum_{c\in\mathcal{I}} f(\rho^c_1) \\ &= \boldsymbol{\gamma}_1\log\boldsymbol{\rho}_1 + \boldsymbol{\gamma}_2\log(\mathbf{1}-\boldsymbol{\rho}_1), \end{aligned} \tag{31}$$

$$\begin{aligned} f(\boldsymbol{a}_1) &= \sum_c f(a^c_{11}) - \frac{1}{\mathcal{T}}U(\boldsymbol{a}_1) \\ &= \boldsymbol{\xi}_{11}\log\boldsymbol{a}_{11} + \boldsymbol{\xi}_{12}\log(\mathbf{1}-\boldsymbol{a}_1) \\ &- \frac{2}{\mathcal{T}}(\log\frac{\boldsymbol{a}_1}{\mathbf{1}-\boldsymbol{a}_1})^{\mathrm{T}}\mathcal{A}\log\frac{\boldsymbol{a}_1}{\mathbf{1}-\boldsymbol{a}_1}, \end{aligned} \tag{32}$$

$$
\begin{aligned}
f(\boldsymbol{a}_2) &= \sum_c f(a_2^c) - \frac{1}{\mathcal{T}} U(\boldsymbol{a}_2) \\
&= \boldsymbol{\xi}_{22} \log \boldsymbol{a}_2 + \boldsymbol{\xi}_{21} \log(\mathbf{1} - \boldsymbol{a}_2) \\
&\quad - \frac{2}{\mathcal{T}} (\log \frac{\boldsymbol{a}_2}{\mathbf{1} - \boldsymbol{a}_2})^{\mathrm{T}} \mathcal{A} \log \frac{\boldsymbol{a}_2}{\mathbf{1} - \boldsymbol{a}_2},
\end{aligned} \tag{33}
$$

$\boldsymbol{\gamma}_i = [\cdots, \gamma_i^c(0), \cdots]$ and $\boldsymbol{\xi}_{ij} = [\cdots, \sum_t \xi_{ij}^c(t), \cdots]$. In (32) and (33), c is not limited in $\mathcal{I}$. For unobserved grid cells, the corresponding elements in $\boldsymbol{\xi}_{ij}$ are set to 0. The derivatives of $Q(\boldsymbol{\theta}, \boldsymbol{\theta}^{(k)})$ with respect to $\boldsymbol{\rho}_1$, $\boldsymbol{a}_1$ and $\boldsymbol{a}_2$ are individually given as

$$
\frac{\mathrm{d}}{\mathrm{d}\boldsymbol{\rho}_1} f(\boldsymbol{\rho}_1) = \boldsymbol{\gamma}_1^{\mathrm{T}} \oslash \boldsymbol{\rho}_1 - \boldsymbol{\gamma}_2^{\mathrm{T}} \oslash (\mathbf{1} - \boldsymbol{\rho}_1), \tag{34}
$$

$$
\begin{aligned}
\frac{\mathrm{d}}{\mathrm{d}\boldsymbol{a}_1} f(\boldsymbol{a}_1) =& \boldsymbol{\xi}_{11}^{\mathrm{T}} \oslash \boldsymbol{a}_1 - \boldsymbol{\xi}_{12}^{\mathrm{T}} \oslash (\mathbf{1} - \boldsymbol{a}_1) \\
&- \frac{4}{\mathcal{T}} \mathcal{A} (\log \frac{\boldsymbol{a}_1}{\mathbf{1} - \boldsymbol{a}_1}) \odot \frac{1}{\boldsymbol{a}_1 \odot (\mathbf{1} - \boldsymbol{a}_1)},
\end{aligned} \tag{35}
$$

$$
\begin{aligned}
\frac{\mathrm{d}}{\mathrm{d}\boldsymbol{a}_2} f(\boldsymbol{a}_2) =& \boldsymbol{\xi}_{22}^{\mathrm{T}} \oslash \boldsymbol{a}_2 - \boldsymbol{\xi}_{21}^{\mathrm{T}} \oslash (\mathbf{1} - \boldsymbol{a}_2) \\
&- \frac{4}{\mathcal{T}} \mathcal{A} (\log \frac{\boldsymbol{a}_2}{\mathbf{1} - \boldsymbol{a}_2}) \odot \frac{1}{\boldsymbol{a}_2 \odot (\mathbf{1} - \boldsymbol{a}_2)},
\end{aligned} \tag{36}
$$

where $\oslash$ is the elementwise division and $\odot$ is Hadamard product. The best estimation of $\boldsymbol{\rho}_1$ is

$$
\boldsymbol{\rho}_1 = \boldsymbol{\gamma}_1^{\mathrm{T}}. \tag{37}
$$

It is not easy to maximize $f(\boldsymbol{a}_1)$ and $f(\boldsymbol{a}_2)$ and a line search method [11] is used to maximize $f(\boldsymbol{a}_1)$ and $f(\boldsymbol{a}_2)$ and obtain the best estimation of parameters in range (0,1).

IV. Simulation

The true map is shown as Figure 3(a). There are 4 square dynamic objects. They have different changing frequencies and their states keep for $\Delta t/3$, $2\Delta t$, $3\Delta t$, $7\Delta t$. The walls on the left are static. The speed is 3 grid cells per δt. At a position, there are four measurement directions: $\pm\pi/2$ and $\pm\pi/4$. They are relative to the robot direction. The maximum range is 8 grid cells. The robot runs near the dashed line randomly 20 loops. The trajectory is shown as Figure 3(b).

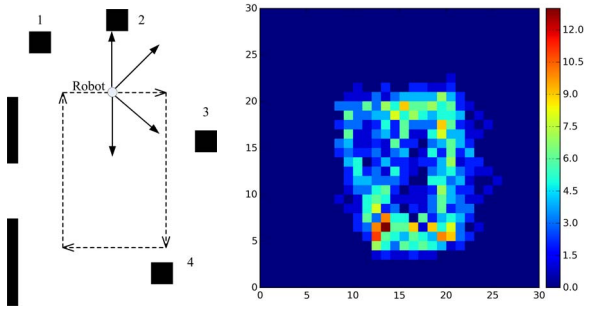

(a) Simulated map (b) Trajectory

Fig. 3: The simulated map and the trajectory

Figure 4(a) represents the times the grid cells are observed. The blue parts are not observed. Figure 4 represents the times the grid cells are observed free. The free space is observed more than once during one loop. Figure 4(b) represents the times the grid cells are observed occupied. Because of the noise of the sensor, the static walls are observed free and the free space around objects are observed occupied sometimes.

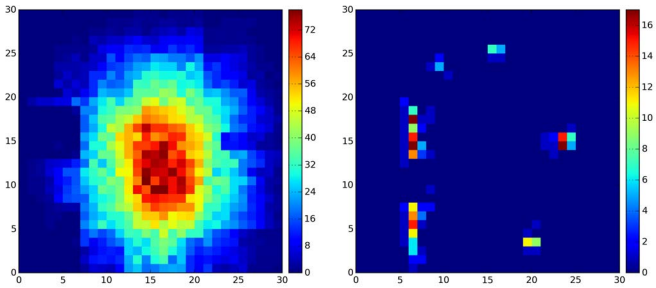

(a) Free (b) Occupied

Fig. 4: The times grid cells are observed free or occupied

The initial parameters $\boldsymbol{a}_1, \boldsymbol{a}_2$, $\boldsymbol{\rho}_1$ are 0.5 and $\mathcal{T} = 50$. The maximum iteration of optimizing process is 300 and the parameter estimation is shown as Figure 5. In Figure 5(a), the observed free space is estimated with low a_{00} and the walls always stay occupied and have high a_{00}. Dynamic object 1 and 2 change fast and the corresponding estimation is low. Dynamic object 3 and 4 stay occupied for a long time and their a_{00} are also high. In Figure 5(b), the free space always stays free and has high a_{11}. The estimations of a_{11} fo the walls, which should be close to 0, are close to 0.4. Because there are fewer free observations for the walls, it is not easy to estimate a_{11}. Given the dependence, their parameters also learn from their neighbours which have high a_{11}. For the dynamic objects, the one with a high changing frequency has a high estimation of a_{11}. The observed space in the centre has more observations, the parameter converges fast and the corresponding parameter are estimated well. The parameter on the border converges slowly.

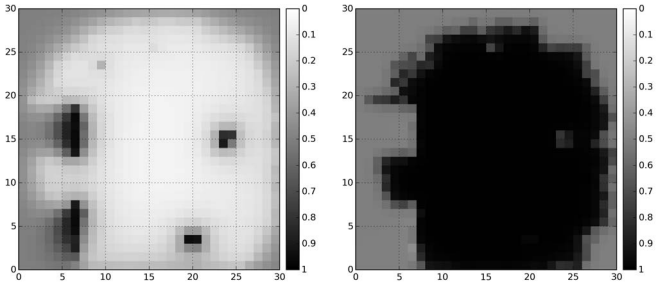

(a) a_{00}: occupied to occupied (b) a_{11}: free to free

Fig. 5: Parameter estimation

V. Conclusions

In this paper, we propose an HMM-based mapping method using MRFs for dynamic environments. An HMM model is built for every grid cell. The MRFs are applied to consider the

dependence between grid cells and the MRF model is built for the whole map. EM algorithm is used to train the HMM parameters. The simulation demonstrates that the proposed method can ensure smooth estimation. However, it takes a long time to estimate the parameters. In the future, we will improve this work to be an online method and implement it in path planning for mobile robots.

REFERENCES

[1] L. R. Rabiner, "A tutorial on hidden markov models and selected applications in speech recognition," *Proceedings of the IEEE*, vol. 77, no. 2, pp. 257–286, 1989.

[2] D. Meyer-Delius, M. Beinhofer, and W. Burgard, "Occupancy grid models for robot mapping in changing environments," in *Proceedings of the Twenty-Sixth AAAI Conference on Artificial Intelligence*, 2012.

[3] H. Moravec and A. Elfes, "High resolution maps from wide angle sonar," in *Proceedings of the IEEE International Conference on Robotics and Automation*, vol. 2, pp. 116–121, IEEE, 1985.

[4] M. Rapp, K. Dietmayer, M. Hahn, B. Duraisamy, and J. Dickmann, "Hidden markov model-based occupancy grid maps of dynamic environments," in *Proceedings of the 19th International Conference on Information Fusion (FUSION)*, pp. 1780–1788, IEEE, 2016.

[5] M. Luber, K. O. Arras, C. Plagemann, and W. Burgard, "Classifying dynamic objects," *Autonomous Robots*, vol. 26, no. 2-3, pp. 141–151, 2009.

[6] G. D. Tipaldi, D. Meyer-Delius, and W. Burgard, "Lifelong localization in changing environments," *The International Journal of Robotics Research*, vol. 32, no. 14, pp. 1662–1678, 2013.

[7] C. Bibby and I. Reid, "Simultaneous localisation and mapping in dynamic environments (slamide) with reversible data association," in *Proceedings of Robotics Science and Systems*, vol. 117, p. 118, 2007.

[8] Z. Wang, R. Ambrus, P. Jensfelt, and J. Folkesson, "Modeling motion patterns of dynamic objects by iohmm," in *Proceedings of the IEEE/RSJ International Conference on Intelligent Robots and Systems*, pp. 1832–1838, IEEE, 2014.

[9] Y. Bengio and P. Frasconi, "An input output hmm architecture," in *Advances in neural information processing systems*, pp. 427–434, 1995.

[10] A. Dadhich, N. Koganti, and T. Shibata, "Modeling occupancy grids using edhmm for dynamic environments," in *Proceedings of the 2015 Conference on Advances In Robotics*, p. 60, ACM, 2015.

[11] S. Wright and J. Nocedal, "Numerical optimization," *Springer Science*, vol. 35, no. 67-68, p. 7, 1999.